AN UNSYMMETRICAL FRACTURE PROCESS ZONE MODEL AND ITS APPLICATION TO THE PROBLEM OF A RADICAL CRACK WITH AN INCLUSION IN LONGITUDINAL SHEAR DEFORMATION

M. Zhu and W. V. Chang
Department of Chemical Engineering
University of Southern California
Los Angeles, CA90089-1211

Abstract
Unsymmetrical crack problems are important for brittle materials such as concrete and brittle polymers. In this paper, by defining a new stress function which is a weight integral of the classical complex stress function over the fracture process zones at two crack tips an unsymmetrical fracture process zone model is developed. As a numerical example, the fracture process zone behavior of a radical crack with an inclusion under longitudinal shear deformation is investigated.
Keywords: Fracture, unsymmetrical fracture process zone

1 Introduction

The distribution of stress in the vicinity of a crack plays a key role

in understanding the fracture behavior of materials. The theory of linear fracture mechanics predicts that stresses approach infinity at the tip of a crack with $r^{-1/2}$ singularity, where r is the distance from the crack tip (Sneddon et al., 1969). But, the singular stress distributions near the crack tip are not realistic, since a real material can only sustain a finite stress before it yields, crazes or cracks. The fracture process zone is a small region surrounding the crack where the fracture develops through the successive stages of inhomogeneous slip, void nucleation, growth and coalescence, and bond breaking on the atomic scale. Dugdale (1960) first developed a continuum mechanics model for the fracture process zone, assuming an elastic-ideally plastic material. In Dugdale model, the fracture process zone is distinguished from the rest of the crack by the action of a constant cohesive stress which resists the crack opening displacement. Dugdale model is only realistic for materials without strain softening or hardening.

Non-metallic materials, such as brittle polymers and concretes, are different from metals in that the stress and strain relation is almost linear until the stress reaches the failure strength, then it drops rapidly with further increases in strain (Peterson, 1981). Dugdale model is not suitable to these materials. Two types of models have been proposed to study the fracture process zone behavior for such cases. The first type includes the fictitious crack model(FCM) by Hillerborg (1980) and the crack band model(CBM) by Bazant and Oh (1983). These models require the fracture energy G_f and the tensile strain-softening curve before numerical simulations of fracture phenomena of the structure are possible. Experimentally, the load-displacement relationship for the whole structure can be easily determined, but this is not the case for the tensile strain softening curve in the process zone. Predicting the structure behavior or to deduce the strain-softening behavior from the structure experiment requires very tedious iterations of numerical simulations.

A different modeling approach was proposed by Duan and Nakagawa (1988) to study the stress distribution in fracture process zone. Their model defines a new complex stress function which is a weight integral of the classical complex stress function over the length of the fracture process zone. Using different weight functions different stress

fields can be analytically determined in the fracture process zone as well as over the whole structure. The boundary conditions are automatically satisfied. Unlike the classical singular solutions, with this new stress function, the crack tip singularity vanishes. Duan and Nakagawa's approach is conceptually simple, direct and elegant. But there are several drawbacks in Duan and Nakagawa's model: (1) The model is in complex plane and this makes the model can only be used for a very small group of simple problems. (2) The model can not take the advantage of large amount of existing approximate singular solutions. (3) The model assumes that both the geometry and the loading conditions are symmetric. But this is not always the case. As well known, most engineering problems are in the unsymmetrical crack problem category due to the unsymmetrical geometry or the unsymmetrical loading conditions. The original Duan and Nakagawa's model has already been reformulated from the complex domain to the real domain by the current authors (Zhu and Chang, 1998). In this paper, with the same weight function idea Duan and Nakagawa employed in their model, an unsymmetrical fracture process zone model is developed. The advantages of this model are: First, all boundary conditions are satisfied automatically in this model. Second, the final model is in the real domain so that it is easy to use. Third, approximate singular solutions can be directly used in this model to simulate the fracture process zone behavior. Forth, the fracture process zone behaviors of different materials can be simulated by choosing different weight functions. As a numerical example, the facture process zone behavior of a radical crack with an inclusion under longitudinal shear deformation is investigated with constant weight function.

2 The Fracture Process Zone Model

In this section, the unsymmetrical fracture process zone model is developed for mode III crack problem. The unsymmetrical fracture process zone model for both mode I and mode II crack problems can be obtained easily by following the same approach. Fig. 1 shows a crack in a solid where c_1 and c_2 are the two crack tips, and b_1 and b_2 the two fracture process zone sizes. When the solid is loaded by far field shearing force τ_∞, which is parallel to the z axis, the resulting

deformation will be anti-plane type. In this case, we have:

$$u = v = 0, \qquad w = w(x, y) \tag{1}$$

where u, v, and w are displacements along the coordinate axes. The nonzero displacement and stress components can be given, in terms of a stress function $F(z, c_1, c_2)$ of the complex variable z=x+iy:

$$\begin{cases} \mu w(x, y) &= Re\{F(z, c_1, c_2)\} \\ \tau_{xz} - i\tau_{yz} &= \frac{dF}{dz} \end{cases} \tag{2}$$

where Re{.} denotes the real part of the function in the brackets and μ is the shear modulus. The boundary conditions of this problem are:

$$\begin{cases} \tau_{yz} &= 0 & y = 0, c_2 < x < c_1 \\ \tau_{yz} &= \tau_\infty & far field \end{cases} \tag{3}$$
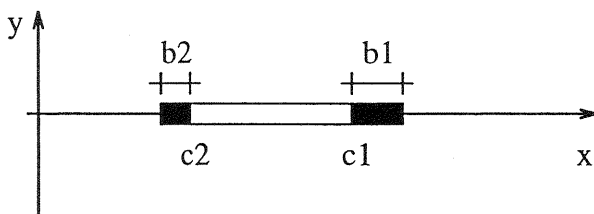

Fig. 1. Crack geometry

The above singular solutions are not realistic near the crack tip because the structure can only sustain finite stress before it yields, crazes or fractures. Researches show that there is a process zone existing at the tip of a crack. If b_1 and b_2 are two fracture process zone sizes at two crack tips as shown in Figure 1, we can define a new stress function as

$$\Phi(z, c_i, b_i) = \int_{c_2-b_2}^{c_2} \int_{c_1}^{c_1+b_1} \rho_1(t_1)\rho_2(t_2)F(z, t_1, t_2)dt_1 dt_2 \tag{4}$$

where $\rho_1(t)$ and $\rho_2(t)$ are two weight functions and satisfy the following equations

$$\begin{cases} \int_{c_2-b_2}^{c_2} \rho_2(t)dt = 1.0 \\ \int_{c_1}^{c_1+b_1} \rho_1(t)dt = 1.0 \end{cases} \tag{5}$$

The stress singularity vanishes with this new stress function and different weight functions will give different stress and displacement

distributions. The stress and displacement components obtained by this new stress function satisfy the following boundary conditions:

$$\begin{cases} \tau_{yz} = 0 & y = 0, \ c_2 \leq x \leq c_1 \\ \tau_{yz} = \tau_\infty & far \ field \\ w = 0 & x \leq c_2 - b_2 \ or \ x \geq c_1 + b_1 \\ w = 0 & |z| = 1 \end{cases} \tag{6}$$

Those two fracture process zone sizes are determined by:

$$\begin{cases} max\{\tau_{yz}(x,0), c_2 - b_2 \leq x \leq c_2\} = \tau_b \\ max\{\tau_{yz}(x,0), c_1 \leq x \leq c_1 + b_1\} = \tau_b \end{cases} \tag{7}$$

where τ_b is the shear failure stress. Substituting the new stress function into Eq. 2 and taking the integration out of the derivative, we can obtain the finite stress concentration solutions as

$$\begin{cases} \tau_{xz} = \int_{c_2-b_2}^{c_2} \int_{c_1}^{c_1+b_1} \rho_1(t_1)\rho_2(t_2)\tau_{xz}^s dt_1 dt_2 \\ \tau_{yz} = \int_{c_2-b_2}^{c_2} \int_{c_1}^{c_1+b_1} \rho_1(t_1)\rho_2(t_2)\tau_{yz}^s dt_1 dt_2 \\ w = \int_{c_2-b_2}^{c_2} \int_{c_1}^{c_1+b_1} \rho_1(t_1)\rho_2(t_2)w^s dt_1 dt_2 \end{cases} \tag{8}$$

where τ_{xz}^s, τ_{yz}^s and w^s are singular solutions of the same problem. From the above equation, we see that both analytical and the approximate singular solutions can be used in this model. Along the crack line, both the stress and displacement components can be calculated by

$$\begin{cases} \tau_{xz}(x,0) = \int_{c_2-b_2}^{c_{20}} \int_{c_{10}}^{c_1+b_1} \rho_1(t_1)\rho_2(t_2)\tau_{xz}^s(x,0) dt_1 dt_2 \\ \tau_{yz}(x,0) = \int_{c_{20}}^{c_2} \int_{c_1}^{c_{10}} \rho_1(t_1)\rho_2(t_2)\tau_{yz}^s(x,0) dt_1 dt_2 \\ w = \int_{c_2-b_2}^{c_{20}} \int_{c_{10}}^{c_1+b_1} \rho_1(t_1)\rho_2(t_2)w^s(x,0) dt_1 dt_2 \end{cases} \tag{9}$$

where:

$$c_{10} = \begin{cases} c_1 & c_2 < x < c_1 \\ x & c_1 < x < c_1 + b_1 \\ c_1 + b_1 & x > c_1 + b_1 \quad or \ x < c_2 - b_2 \end{cases} \tag{10}$$

$$c_{20} = \begin{cases} x & c_2 - b_2 < x < c_2 \\ c_2 & c_2 < x < c_1 \\ c_2 - b_2 & x < c_2 - b_2 \quad or \ x > c_1 + -b_1 \end{cases} \tag{11}$$

It is needed to point out that, in real calculation, we do not need to calculate the new stress function. We can obtain the finite stress concentration solutions directly by doing simple numerical integrations of Eq. 8 and 9 with the classical solutions.

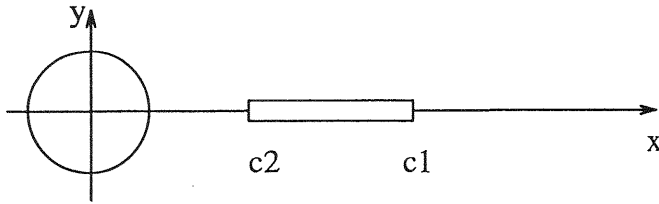# 3 Numerical Examples and Discussion

3.1 Basic Equations

Fig. 2. A radical crack with an inclusion

Fig. 2 shows a solid containing a crack with a rigid inclusion of unit radius. The crack occupies the region $c_2 \leq x \leq c_1$, y=0. The shear modulus μ and the failure stress $= \tau_b$ of the material are 2.5GPa and 10MPa respectively. The solid is loaded by the far field shear stress τ_∞ along z axis. The boundary conditions to be satisfied at the crack and inclusion are

$$
\begin{cases}
\tau_{yz} = 0 & y = 0 & c_2 < x < c_1 \\
w = 0 & y = 0 & x \leq c_2 \ or \ x \geq c_1 \\
w = 0 & |z| = 1 \\
\tau_{yz} = \tau_\infty & far \ field
\end{cases}
\tag{12}
$$

For this typical crack problem, the singular stress function F(z, c_i) satisfying the above boundary conditions is suggested by Sedeckyj (1974):

$$
F(z, c_i) = -iP \left\{ \frac{(z - c_1)(1/z - c_1)(z - c_2)(1/z - c_2)}{c_2^2} \right\}^{\frac{1}{2}}
\tag{13}
$$

The singular solutions along the crack line can be easily obtained when $c_2 \leq x \leq c_1$

$$
\begin{cases}
\tau_{xz}(x,0) = \frac{(x^2-1)p}{2x^2} \left\{ \left[\frac{c_2(c_1-x)(c_1-\frac{1}{x})}{c_1(x-c_2)(c_2-\frac{1}{x})} \right]^{\frac{1}{2}} + \left[\frac{c_1(x-c_2)(c_2-\frac{1}{x})}{c_2(c_1-x)(c_1-\frac{1}{x})} \right]^{\frac{1}{2}} \right\} \\
\tau_{yz}(x,0) = 0 \\
w(x,0) = \frac{p}{\mu} \left\{ \frac{(c_1-x)(c_1-\frac{1}{x})(x-c_2)(c_2-\frac{1}{x})}{c_1 c_2} \right\}^{\frac{1}{2}}
\end{cases}
\tag{14}
$$

When $x > c_1$ or $x < c_2$, we have:

$$
\begin{cases}
\tau_{xz}(x,0) = 0 \\
\tau_{yz}(x,0) = \frac{(x^2-1)p}{2x^2} \left\{ \left[\frac{c_2(x-c_1)(c_1-\frac{1}{x})}{c_1(x-c_2)(c_2-\frac{1}{x})} \right]^{\frac{1}{2}} + \left[\frac{c_1(x-c_2)(c_2-\frac{1}{x})}{c_2(x-c_1)(c_1-\frac{1}{x})} \right]^{\frac{1}{2}} \right\} \\
w(x,0) = 0
\end{cases}
\tag{15}
$$

1102

The unsymmetrical fracture process zone solutions along the crack line can be obtained by substituting Eq. 14 and 15 into Eq. 9 where $\rho_1(t) = 1/b_1$ and $\rho_2(t) = 1/b_2$

$$\tau_{xz}(x,0) = \frac{(x^2-1)P}{2b_1 b_2 x^2} \int_{c_2-b_2}^{c_{20}} \int_{c_{10}}^{c_1+b_1} \left\{ \left[\frac{t_2(x-t_1)(t_1-1/x)}{t_1(x-t_2)(t_2-1/x)} \right]^{\frac{1}{2}} \right.$$
$$\left. + \left[\frac{t_1(x-t_2)(t_2-1/x)}{t_2(x-t_1)(t_1-1/x)} \right]^{\frac{1}{2}} \right\} dt_1 dt_2 \tag{16}$$

$$\tau_{yz}(x,0) = \frac{(x^2-1)P}{2b_1 b_2 x^2} \int_{c_{20}}^{c_2} \int_{c_1}^{c_{10}} \left\{ \left[\frac{t_2(x-t_1)(t_1-1/x)}{t_1(x-t_2)(t_2-1/x)} \right]^{\frac{1}{2}} \right.$$
$$\left. + \left[\frac{t_1(x-t_2)(t_2-1/x)}{t_2(x-t_1)(t_1-1/x)} \right]^{\frac{1}{2}} \right\} dt_1 dt_2 \tag{17}$$

$$w(x,0) = \frac{P}{\mu b_1 b_2} \int_{c_2-b_2}^{c_{20}} \int_{c_{10}}^{c_1+b_1} \left\{ \frac{(t_1-x)(t_1-1/x)}{t_1} \right.$$
$$\left. \frac{(x-t_2)(t_2-1/x)}{t_2} \right\}^{\frac{1}{2}} dt_1 dt_2 \tag{18}$$

When c_2 approaches the inclusion, the left crack tip will be arrested and the solution can be obtained by letting c_2 go to the inclusion

$$\left\{ \begin{array}{l} \tau_{xz}(x,0) = \kappa \int_{c_{10}}^{c_1+b_1} \left\{ \left[\frac{c_2(x-t)(t-1/x)}{t(x-c_2)(c_2-1/x)} \right]^{\frac{1}{2}} + \left[\frac{t(x-c_2)(c_2-1/x)}{c_2(x-t)(t-1/x)} \right]^{\frac{1}{2}} \right\} dt \\ \tau_{yz}(x,0) = \kappa \int_{c_1}^{c_{10}} \left\{ \left[\frac{c_2(x-t)(t-1/x)}{t(x-c_2)(c_2-1/x)} \right]^{\frac{1}{2}} + \left[\frac{t(x-c_2)(c_2-1/x)}{c_2(x-t)(t-1/x)} \right]^{\frac{1}{2}} \right\} dt \\ w(x,0) = \frac{P}{\mu b_1} \int_{c_{10}}^{c_1+b_1} \left\{ \frac{(t-x)(t-1/x)}{t} \frac{(x-c_2)(c_2-1/x)}{c_2} \right\}^{\frac{1}{2}} dt \end{array} \right. \tag{19}$$

where $\kappa = (x^2-1)p/(2b_1 x^2)$

3.2 Numerical Results and Discussion

In this subsection, with constant weight functions, we first study the fracture process zone behaviors of the above mentioned problem. Then, the crack-inclusion interaction is briefly discussed.
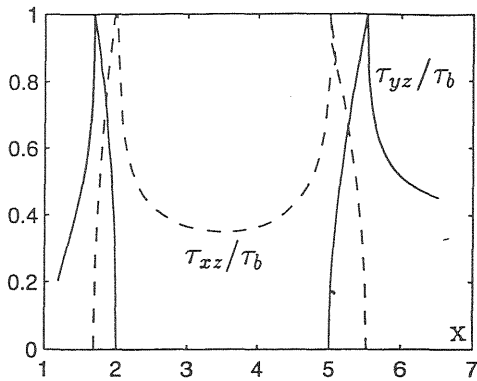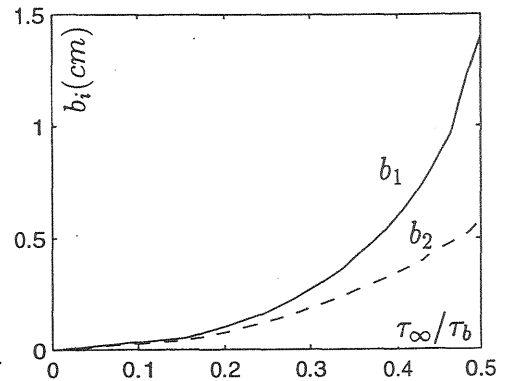

Fig. 3. Stress distributions

Fig. 4. b vs τ_∞ curve

Fig. 3 shows the shear stress distributions (τ_{xz}, τ_{yz}) along the crack line when c_1=5cm, c_2=2cm and the far field shear stress τ_∞=0.4τ_b. The curve tells us that τ_{xz} reaches its maximum at crack tips c_1 and c_2, but τ_{yz} reach their maximum at the ends of the process zone. Fig. 4, 5, and 6 show how fracture process zone sizes b_i, crack tip opening displacements $CTOD_i$ and the J integers J_i (i=1,2) change with the increase of τ_∞. We see that the left crack tip is much weaker than the right tip even though b_i, $CTOD_i$ and J_i increase with τ_∞. The unsymmetrical characteristics can not be ignored.
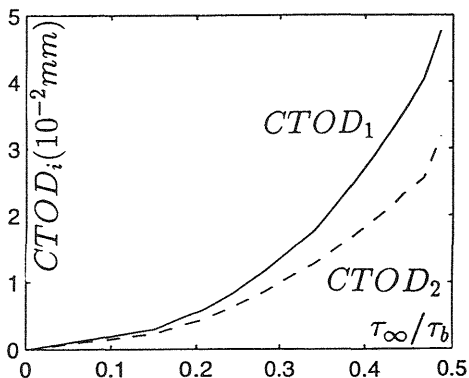

Fig. 5. CTOD vs τ_∞ curve   Fig. 6. J integer vs τ_∞ curve
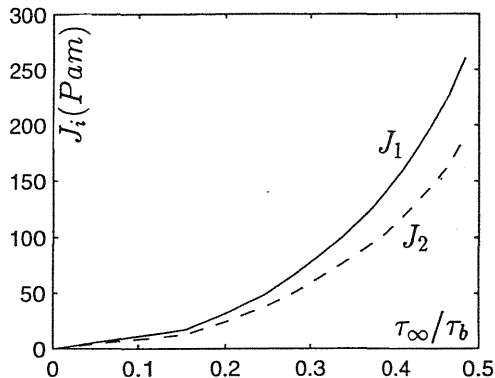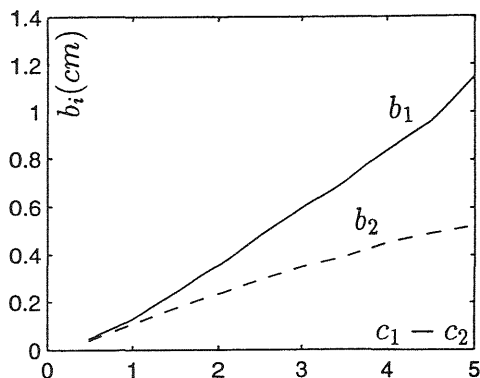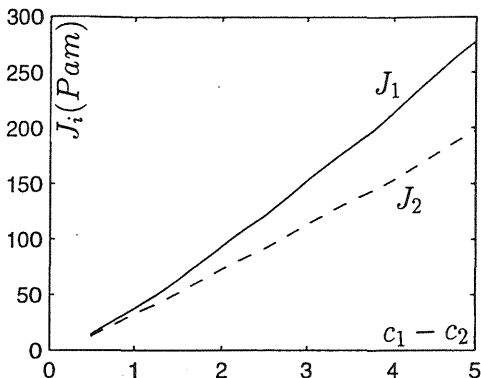

(a) b_i vs crack length curve   (b) J_i vs crack length curve

Fig. 7. Type one interaction results

Two kinds of crack-inclusion interactions are discussed with fixed far stress ($\tau_\infty = 0.4\tau_b$): (1) The left crack tip c_2 is fixed (c_2=2cm) and the crack length changes; (2) The crack length is fixed ($c_1 - c_2$=3cm) but the left crack tip moves towards the inclusion. Figure 7 shows

the results of the first type of crack-inclusion interaction. Fig. 7 tells that, when the crack length increases, both b_i and J_i increases. Then, it also shows that both J_1 and J_2 are almost linear with the crack length. The results of the second type of crack-inclusion interaction is shown in Fig. 8. It tells that, when c_2 approaches the infinity, the unsymmetrical characteristics tend to disappear. Then, it also tell us that, when c_2 goes to the inclusion, b_2 tends to go to zero. This is because the analytical solution assumes the inclusion rigid and this makes the inclusion sustain all the load when the crack's left tip is on the inclusion's surface.
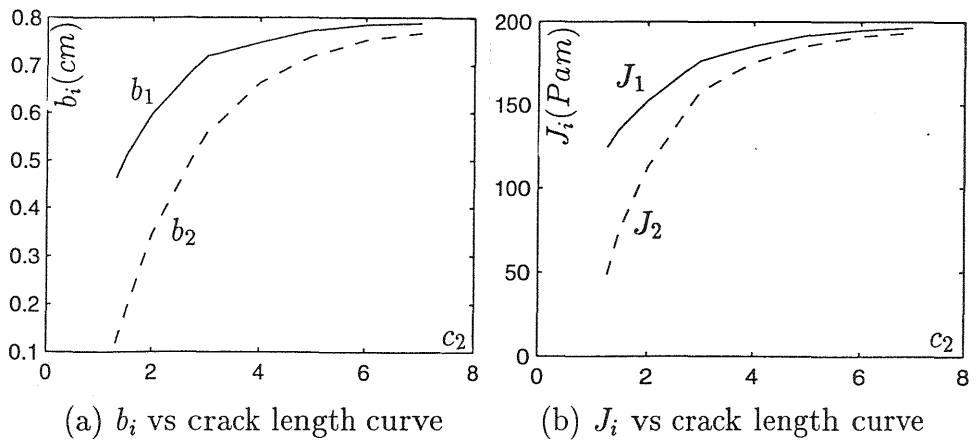

(a) b_i vs crack length curve (b) J_i vs crack length curve

Fig. 8. Type two interaction results

4 Conclusion

In the present paper, by defining a new stress function which is a weight integral of the classical complex stress function over the length of two fracture process zones, a unsymmetrical fracture process zone model is developed. The advantages of this model are: (1) All boundary conditions are satisfied automatically in this model. (2) The final model is in the real plane so that it is easy to use. (3) Approximate singular solutions can be directly used in this model to simulate the fracture process zone behavior. (4) The fracture process zone behaviors of different materials can be simulated by choosing different weight functions. As a numerical example, the facture process zone behavior of a radical crack with an inclusion under longitudinal shear deformation is studied.

References

Sneddon, I. N., and Lowengrub, M. (1969) **Crack problems in the classical theory of elasticity**, John Wiley and Sons.

Dugdale, D. S. (1960) Yielding of Steel sheets containing slits, **J. Mech. Phys. Solids**, 8, 100-104.

Peterson, P. E. (1981), Crack growth and development of fracture zones in plain concrete and similar materials, **Report TVBM-1001, Decision of Building Materials**, Lund Institute of Technology, Sweden.

Hillerborg, A. (1980) Analysis of fracture by means of the fictitious crack model, particularly for fiber-reinforced concrete, **Int. J. Cement Compos.**, 2, 177-184.

Bazant, Z. P. and Oh, B. H. (1983) Crack band theory for fracture of concrete, **Mater. Structure**, 16, 155-177.

Duan, S. J., Nakagawa, K. (1988) Stress functions with finite stress concentration at the crack tips for central cracked panel, **Engng Fracture Mech.**, 29(5), 517-526.

Zhu, M. and Chang, W. V. (1998) A new formulation of Duan and Nakagawa's fracture process zone model and its application to an infinite row of collinear cracks, **The 12th ASCE Engineering Mechanics Conference**, San Diego(to appear).

Sendeckyj, G. P. (1974) Interaction of cracks with rigid inclusions in longitudinal shear deformation, **Int. J. of Fracture**, 10(1), 45-52.